

9/13/11

Revised

Ignition and Combustion of Aluminum in Oxygen/Nitrogen

Mixture Streams

Accepted  
for QF

gt/g

Saburo YUASA, Yuxiu ZHU and Sakurako SOGO

Original

Tokyo Metropolitan Institute of Technology

with

Asahigaoka 6-6, Hino, Tokyo 191, JAPAN

figures

-----  
Corresponding Author:

Name; S. YUASA

Address; Tokyo Metropolitan Institute of Technology

Department of Aerospace Engineering

Asahigaoka 6-6, Hino-city, Tokyo 191, JAPAN

TEL ; 0425-83-5111 ext 3506

FAX ; 0425-83-5119

-----  
Shortened running title:

Ignition and Combustion of Al

## Abstract

The ignition and combustion of a solid cylinder of Al was studied experimentally by using the stagnation region of impinging  $O_2/N_2$  (20/80) mixture streams over a wide range of pressure and velocity of the streams. When an original oxide coating did not exist on the Al surface, the critical spontaneous ignition temperatures were lower than the melting point of  $Al_2O_3$ , decreasing with reduction in pressure and velocity of the streams. Whether surface reactions initially formed a protective  $Al_2O_3$  film on the surface or not decided the ignition, leading to the development of a luminous diffusion flame. When the Al surface was covered with an original oxide coating, it was observed that ignition occurred in the gas phase at the instant of the breaking of the coating. During combustion, the Al surface remained clean or covered with porous deposits.  $AlO$  was produced in the gas phase through the reactions of Al vapor with  $O_2$ . The  $AlO$  had a peak concentration in the gas phase away from the surface.  $Al_2O_3$  also condensed in the gas phase.  $N_2$  in the mixtures was found not to affect the ignition and combustion process due to much less reactivity with Al. The combustion mechanism for the  $Al-O_2/N_2$  system has been postulated, including the surface and gas-phase reactions producing Al vapor,  $AlO$ ,  $Al_2O$ ,  $AlO_2$ ,  $O$  and condensed  $Al_2O_3$ . The ignition mechanism is also discussed.

## 1. Introduction

The very high heat of combustion of Al has directed our interest to increasing rocket performance using Al containing propellants that elevate the flame temperature. This has led to numerous studies on ignition and combustion of Al particles and wires in oxidizing atmospheres [1-4]. Since an  $\text{Al}_2\text{O}_3$  film has a protective nature for further oxidation, several investigators pointed out that the ignition of Al will occur when its protective nature ceases after the melting of the oxide [1,5]. Merzhanov et al.[4], using electrical heating wires, have observed that the ignition temperatures of Al were either equal to or markedly lower than the melting point of  $\text{Al}_2\text{O}_3$ . A consideration of the physical properties of Al and the spectral results showed that Al burns in the gas phase with a diffusion flame [2,6]. In spite of intense research efforts, details of the ignition and combustion process remain obscure because of difficulties in measuring Al temperatures due to the extremely high ignition temperature and in observing details of burning thin wires and small particles. The formation of a condensed oxide and many gaseous sub-oxides in the flame further complicates combustion kinetic processes of Al with oxidizers [7,8]. The authors know of no experimental work that has reported on the structure of Al diffusion flames in  $\text{O}_2$ -containing atmospheres. A knowledge of the structure is very important for developing theoretical models of Al combustion.

The present experimental study was made to investigate spontaneous ignition temperatures, the ignition process and flame structure of Al in  $\text{O}_2/\text{N}_2$  mixture streams. In the experiment, a stagnation region of an impinging  $\text{O}_2/\text{N}_2$  stream, in the same manner as that of our previous studies [9,10], was adopted to facilitate the experimental observation and to simplify the flow field. For comparison purpose, the experiment with an original

oxide coating on Al surface was also performed.

## 2. Experimental Apparatus and Procedure

Figure 1 shows a schematic of the experimental apparatus. This is essentially the same as that specified in the previous paper [10]. A sample holder made of  $\text{Al}_2\text{O}_3$  was situated 14 mm downstream of  $\text{O}_2/\text{N}_2$  streams ejected through a nozzle 25 mm in diameter. The ejection velocities  $V_m$  of the  $\text{O}_2/\text{N}_2$  streams were varied within a range from 0.5 to 5.0 m/s at ambient chamber pressures  $P_m$  from 8 to 101 kPa. An Al sample (purity: 99.99% or higher) 10 mm in diameter and 10 mm in depth was inserted into a depression of the sample holder. In the case without an original oxide coating, like conventional experiments [9,10], a method was adopted for replacing an Ar stream with an  $\text{O}_2/\text{N}_2$  stream when a predetermined sample temperature was reached. On the other hand, in the case with an original oxide coating, heating was initiated at room temperature in an  $\text{O}_2/\text{N}_2$  stream at a predetermined pressure and stream velocity, and continued until ignition occurred. In this experiment, the oxygen mole fraction  $X_{\text{O}_2}$  in the  $\text{O}_2/\text{N}_2$  mixtures was constantly maintained at 0.2.

In the case without an original oxide coating, a calibrated radiation thermometer was used to measure the Al sample temperature in Ar [10]. To measure the temperature of an Al sample with an original oxide coating formed thereon, a radiation thermometer and a chromel-alumel thermocouple were used simultaneously. According to this method, an accurate temperature could be measured to around 1400°C at which the thermocouple fuses. Temperatures higher than this were measured by using only the radiation thermometer, assuming that the relation between these two temperatures holds even at 1400°C or higher. Continuous photography

with a video, filtered photographs having specific wavelengths and spectral measurement were executed synchronously through quartz windows. Condensed combustion products gathered after the experiment were analyzed by X-ray diffractometry.

### 3. Experimental Results

#### 3.1 Ignition

In this experiment, the sample temperature at the instant of replacement of an Ar stream by an  $O_2/N_2$  stream was defined as the initial sample temperature  $T_{in}$ . A moment of appearance of a flame was defined as ignition, and a lowest initial sample temperature above which a sample heated up by itself to ignition was defined as the spontaneous critical ignition temperature  $T_{cr}$ .

##### 3.1.1 Without an original oxide coating

###### i) Ignition process

All samples used in this study had a "natural" (very thin) oxide coating at room temperature. When the sample was heated in an Ar stream, the "natural" oxide coating broke at about 1000 °C due to the convection of liquid Al. After the break of the "natural" coating, the metal surface was kept clean. Thus we call this case the sample without an original oxide coating. The sample actively ejected Al vapor, which was condensed in the open space above the surface to form a stagnation stream line. (This was confirmed by X-ray diffractometer analysis of the condensed particles gathered during the heating stage in the Ar stream.) The vapor was visible above the sample temperature of about 1400 °C. As soon as the sample was exposed to the  $O_2/N_2$  stream, the production of the white smoke of the condensed Al vapor was

stopped. When ignition occurred, the gas phase near the sample surface started to emit light uniformly. Simultaneously, Al lines and AlO bands appeared. As time went on, the emission in the gas phase became stronger, leading to combustion with a fully developed flame. It was found throughout this process that no reaction film was formed on the surface. Also, it was confirmed that the qualitative ignition behavior mentioned above did not vary within the range of the pressure and velocity tested. On the other hand, in the case of non-ignition, although the emission near the sample surface became temporarily stronger just after exposure to the  $O_2/N_2$  stream, the sample surface was immediately covered with a reaction film and the emission vanished, resulting in non-ignition. This suggests that the film inhibited further oxidation. The present experimental results confirmed that the ignition process in the  $O_2/N_2$  streams was essentially the same as that in the  $CO_2$  streams described in the previous paper [10], and whether a protective reaction film was formed at the beginning of the ignition process or not controlled the process.

ii) Spontaneous critical ignition temperature

The ignition delay time was defined as an interval to ignition after the gas replacement of Ar by an  $O_2/N_2$  stream had taken place. The delay time varied little with  $T_{in}$ , always being 0.5-1.2 sec. When  $T_{in}$  was below a certain critical temperature, ignition could not occur. Such a tendency and the order of delay time were the same independent of variations in  $P_m$  and  $V_m$  within the experimental range. This behavior was the same as that of Al in the  $CO_2$  streams [10], and implies that the ignition process of Al in  $O_2/N_2$  streams was not controlled by heat accumulation through the reaction process [9,10]. Figure 2-(1) shows a varia-

tion of  $T_{cr}$  with  $P_m$ , and Fig.2-(2) a variation of  $T_{cr}$  with  $V_m$ . These figures show that  $T_{cr}$  increased with an enlargement in  $P_m$  and  $V_m$ . The tendencies of these two were also the same as that in the  $CO_2$  streams [10]. Yet the values of  $T_{cr}$  were substantially the same as those in the  $CO_2$  streams. It should be noted that  $T_{cr}$  values were much lower than the melting point of  $Al_2O_3$ , 2042 °C, which was reported as the ignition temperature of Al with an initial oxide coat on it in oxidizing atmospheres [2,4].

### 3.1.2. With an original oxide coating

#### i) Ignition process

When the sample with a "natural" oxide coating was heated in the  $O_2/N_2$  stream, the sample was further oxidized to increase the thickness of the oxide coating. In this case the sample was originally covered with an oxide coating. Figure 3 shows typical time variation of the sample appearances and emission spectra leading to ignition at low pressures. Figure 3(a) shows Al immediately before ignition, having the surface covered with an original oxide coating. In Fig. 3(b), 0.34 sec later, the coating began to be broken on the circumference of the sample surface, and weak emission was visible in the gas phase near the broken place according to the observation from the side. (In Fig.3 the side photographs at (a) and (b) were treated with image enhancement to recognize the emission clearly.) However, no variation appeared yet in the emission spectra due to its weakness. As time went on, the broken film area was enlarged as shown in Fig.3(c). This was followed by the increase in emission intensity in the gas-phase, with a corresponding appearance of Al and AlO spectrum. About three seconds later, the whole reaction films on the surface were perfectly broken to expose a metallic surface of Al. Finally a stable diffusion flame of Al

vapor, as shown in Fig. 3(d), was formed. Such behavior was basically observed when the heating rate (to be mentioned later) was fast at low pressures. In the case of slow heating rates or high ambient pressures, the coating was not perfectly broken, and a large quantity of irregularities appeared on the surface. Following this, a flame developed over it.

## ii) Ignition temperature

It was observed that when the reaction film was broken, Al vapor was ejected in the gas phase, leading to ignition. The ignition temperature  $T_{ig}$  in Fig. 3(b) was 1934°C. Figure 4 shows a variation of  $T_{ig}$  with the heating rate Hr defined as  $[(T_{ig}-660)/(\text{the time interval from a finish of melting to ignition}) \text{ [}^\circ\text{C/s]}]$ .  $T_{ig}$  clearly decreased with increasing Hr. When Hr was slow,  $T_{ig}$  was close to the melting point of  $\text{Al}_2\text{O}_3$ . Also, it was found that  $T_{ig}$  remained unchanged irrespective of the ambient pressure. This suggests that the breaking mechanism of the original oxide coating was almost insensitive to pressure within the range of our study.

## 3.2 Combustion

### 3.2.1 Combustion process

At low pressures, a stable flame as shown in Fig. 3(d) was formed after ignition for the cases without an original oxide coating or with it at high heating rates. The combustion continued for several minutes. The portion that was emitting light very brightly was composed of fine particles of  $\text{Al}_2\text{O}_3$  condensed in the gas phase. Since the particles were convected away by the bulk gas flow, this emission area represented a stagnation

point region. A distance between the Al surface and the stagnation point was about 1.8 mm in the case of Fig.3(d). The ejection velocity of Al vapor  $V_v$  was roughly estimated from an inferred position of the stagnation point by assuming no surface reactions, a reasonable gas density close to the surface and the relation  $V_v = V_m \sqrt{h_v/h_m}$ , where  $h_v$  is the distance between the Al surface and the stagnation point and  $h_m$  is the distance between the nozzle exit and the stagnation point. The velocity was about 0.34 m/s. It was observed that the distance was gradually increased as combustion continued, and that it was a maximum of about 6 mm at  $P_m = 8$  kPa and  $V_m = 2$  m/s. This suggests that the sample temperature was increased with the progress of combustion. During combustion, the metal surface was exposed, and any deposit of combustion products was not visible. This observation leads to a conclusion that  $O_2$ , which would react on the Al surface to produce  $Al_2O_3$  film, did not reach the surface. The burning rate of Al also was roughly estimated from the ejection velocity of Al vapor. The rates were about 0.5- 1.3 mg/(cm<sup>2</sup>.s), which are several times larger than Al in CO<sub>2</sub> streams [10].

When the heating rate was slow for Al samples with an original oxide coating, red-hot combustion products were irregularly deposited on the sample surface, and the combustion proceeded over the deposits as shown in Fig.5. This shows that the gaseous combustion products produced in the gas phase could diffuse back to the surface and form the deposits, which were porous. However, for Al without an original oxide coating, no deposit was visible on the surface even at high pressures.

### 3.2.2 Flame spectrum and combustion products

In the emission spectrum of a burning Al sample in the O<sub>2</sub>/N<sub>2</sub> stream, the atomic lines of Al, the bands of AlO and the

continuum emission were clearly visible irrespective of the presence or absence of the deposits on the Al surface. Any spectra related to AlN were not observed. The features of these spectra did not change with the ambient pressure, but had quite the same behavior as that of emission spectra of Al flames in the CO<sub>2</sub> streams [10]. The analysis of condensed combustion products in the gas phase showed that AlN was slightly detected in addition to Al<sub>2</sub>O<sub>3</sub>. However, no AlN was detected from a reaction film formed on the surface during the ignition process.

In order to confirm the reactivity of Al with N<sub>2</sub>, an additional experiment of an Al sample without an original oxide coating was conducted in a pure N<sub>2</sub> stream. As a result, although the sample with a clean surface continued to generate white smoke vigorously, no combustion occurred even at 2000 °C. AlN was slightly identified in the condensed smoke. These experimental results indicate that although N<sub>2</sub> could react with Al vapor in the gas phase, the reaction rate was exceedingly slow, and it hardly reacted with liquid Al on the surface. Therefore, a gas-phase reaction process between Al vapor and O<sub>2</sub> is essentially important in the combustion process of Al in the O<sub>2</sub>/N<sub>2</sub> streams.

### 3.2.3 Flame structure

In order to investigate the flame structure of Al in the O<sub>2</sub>/N<sub>2</sub> streams, simultaneous photographs for the same flame having a wide emission zone at low pressures were taken on infrared films through interference and bandpass filters. Figure 6-(1) shows typical filtered photographs. Figure 6-(2) shows corrected emission intensity distributions along the paths drawn in the photographs. The emission intensities passing through the filters for Al lines and AlO bands contained luminous elements resulting from the continuum. In addition, since the flame

formed on the Al convex surface was not one dimensional, an emission intensity in which light in the depth direction had been integrated was recorded in the photographs. Therefore, in order to know a true intensity distribution, it is necessary to eliminate the continuous light elements, and to consider the effect of three-dimensional property of the flame. The continuous light elements superimposed on Al and AlO emissions were deducted using the intensities of the pure continuum emissions obtained at the wavelengths near the Al lines or AlO bands. (Filter photographs of Fig. 6-(1) show that the outer regions of the uncorrected Al and AlO emissions with continuous light were located in the luminous region of the pure continuum. In this region, the intensity of the continuous light elements superimposed on Al and AlO emissions was found to be much higher than those of pure Al and AlO emissions. Thus it was very difficult to subtract accurately the superimposed continuous light elements from the Al and AlO emissions. This indicates that the outer positions of the pure Al and AlO emissions in Fig. 6-(2) had some inaccuracy.)

Concerning the correction of the effect of the three-dimensional property, we derived the true intensity distributions assuming point symmetric concentrations of Al, AlO and condensed  $Al_2O_3$  over the Al surface and using the method of Abel's integral equation, in a similar way as was done for an axisymmetric diffusion flame by South and Hayward [11].  $R_i(r)$ , the true emission intensity distribution of  $i$  species, is analytically given by

$$R_i(r) = -\frac{1}{\pi} \int_r^{r_{ei}} \frac{(dI_i(x) / dx)}{\sqrt{x^2 - r^2}} dx$$

where  $I_i(x)$ : the measured emission intensity distribution of  $i$  species as a function of  $x$ ,  $x$ : the axis perpendicular to the

emission beam, equal to the pass shown in the photographs,  $r$ : the radius from the center of symmetry,  $r_{ei}$ : the radius of the outer edge of emission of  $i$  species. Figure 6-(2) shows ultimately derived intensity distributions for Al, AlO and the continuum.

The intensity distribution of the continuum shows that condensation of  $\text{Al}_2\text{O}_3$  occurred vigorously in an open space about 4 mm away from the surface. Since the condensation reactions involve a great deal of heat generation, it is predicted that the temperature in this area was highest. Comparing with the continuum, both the emission intensities of Al and AlO have the maximum luminosity in the gas phase near about 2-3 mm away from the surface. The peak of Al was slightly nearer to the surface. Regarding AlO, this suggests that AlO was produced in the gas phase on the metal side rather than at the position where the condensation of  $\text{Al}_2\text{O}_3$  occurred, diffusing towards the surface and outwards. Since the emission of Al may be due to chemiluminescent excitation [12,13], the intensity distribution of Al vapor is considered to represent the concentration of excited Al atoms depending on the temperature in the flame and on the concentration of Al vapor. In addition, since there was no or little contribution due to reactions of Al vapor with nitrogen, this structure can be said to have essentially the same structure as that of Al flames in the  $\text{CO}_2$  streams [10].

#### 4. Discussion

##### 4.1. Combustion Process

The present experimental results have revealed that in  $\text{O}_2/\text{N}_2$  (20/80) mixture streams the combustion behavior of Al without an

original oxide coating and with it at high heating rates and low pressures was similar to that of Al in the CO<sub>2</sub> streams [10]. This suggests that an analogy between Al combustion mechanisms in O<sub>2</sub> and in CO<sub>2</sub> may be valid. From the results and the possible kinetics of Al with O<sub>2</sub> proposed by other investigators [7,8,14], we suggest the following kinetic scheme:

Reaction	Heat of Reaction [kJ] [15]
On the surface	
Al(l) -->Al(g)	+ 317.7      ①.
AlO+Al(l) -->Al <sub>2</sub> O	- 224.0      ②.
In the gas phase	
Al(g)+O <sub>2</sub> -->AlO+O	+ 6.53      ③.
Al(g)+O+M -->AlO+M	- 492.1      ④.
AlO+O <sub>2</sub> -->AlO <sub>2</sub> +O	- 78.6      ⑤.
AlO+AlO <sub>2</sub> -->Al <sub>2</sub> O <sub>3</sub> (l)	-1557.2      ⑥.
Al <sub>2</sub> O+O <sub>2</sub> -->Al <sub>2</sub> O <sub>3</sub> (l)	-1562.2      ⑦.
O+O+M -->O <sub>2</sub> +M	- 498.7      ⑧.

With respect to the condensation of Al<sub>2</sub>O<sub>3</sub>, Henderson [16] has proposed a series of polymerization reactions of AlO to (AlO)<sub>n</sub> followed by ejection of Al(g) through the reaction [(AlO)<sub>n</sub> -> (Al<sub>2</sub>O<sub>3</sub>)<sub>n/3</sub>(l)+n/3xAl(g)]. King [17] pointed out that since the polymerization is a complex multi-step scheme, consequently it is probably slow. If so, the concentration of (AlO)<sub>n</sub> must be sufficiently large to form Al<sub>2</sub>O<sub>3</sub>(l). However, the equilibrium concentration of (AlO)<sub>2</sub> is two or three orders in magnitude smaller than those of Al<sub>2</sub>O and AlO<sub>2</sub> [18]. In the Henderson's paper, the author suggested that AlO formed through

the reaction  $[Al_2O+O_2 \rightarrow (AlO)_2+O]$ . The Gibbs free energy changes of this reaction at high temperatures give positive values [15], which means that this reaction cannot proceed spontaneously. This consideration leads to the conclusion that the polymerization process seems not to be important for giving  $Al_2O_3(l)$  in steady  $Al/O_2/N_2$  flames.

In view of the above considerations, we postulated a combustion mechanism shown schematically in Fig. 7. In this mechanism, we neglect any reaction of Al with  $N_2$  due to quite low reaction rate. Although this mechanism is somewhat speculative because of uncertainty of the reaction kinetics and the lack of information on the reaction rates, it can give a consistent full explanation of the observed experimental results and the equilibrium compositions of  $Al-O_2/N_2(20/80)$  flames calculated by Ref. 18. Since Al has a high vapor pressure above  $T_{cr}$ , for example about 8.3 kPa at the melting point of  $Al_2O_3$  2042 °C, it vaporizes vigorously and reacts with  $O_2$  in the gas phase, producing AlO. Simultaneously, the conversion of AlO to condensed  $Al_2O_3$  particles occurs by way of the formation of  $AlO_2$ . (In many previous studies for Al combustion,  $Al_2O_3$  vapor has never been detected.) The condensed particles follow the bulk gaseous motion in the stagnation region to form a stagnation stream line. Although AlO diffusing back to the Al surface forms  $Al_2O$  on it, the absence of any  $O_2$  close to the surface inhibits the formation of an  $Al_2O_3$  film. Since the theoretical flame temperature of  $Al-O_2/N_2(20/80)$  system at the stoichiometric ratio is 3295 °C at 101 kPa [18], mainly attributed to Reactions 6 and 7, both of which form condensed  $Al_2O_3$ , the temperature distribution in the gas phase has a peak away from the surface as shown in Fig.7.

On the other hand, when Al burned on the deposit surface, the observed combustion behavior changed in comparison to the

behavior without deposit. However, the appearances of the burning samples and the spectrum observation, here and the previous works [1,2,6], suggest that the Al sample burned in the gas-phase. Evidences lead to the conclusion that although the deposit restricts the combustion reactions close to the surface, the combustion mechanism of Al with deposit is essentially identical with that suggested for Al without deposit. In this case, an additional oxide accumulation at the surface may be explained as follows. Intermediate gaseous combustion products AlO and AlO<sub>2</sub> can easily diffuse toward the Al surface. In addition, the concentration of oxygen diffusing from the upstream through the reaction region increases considerably close to the Al surface. These species react on the initial oxide surface by Reactions 6 and 7 to form the deposit of condensed Al<sub>2</sub>O<sub>3</sub>, which accumulates during combustion. The difference in the position where the reactions occurred makes the appearance of the physical combustion processes different.

#### 4.2. Ignition Process

##### 4.2.1. Without an original oxide coating

We found that in the case of ignition without an original oxide coating a diffusion flame of Al vapor with O<sub>2</sub> was developed surrounding a clean Al surface in O<sub>2</sub>/N<sub>2</sub>(20/80) mixture streams. On the contrary, once an Al<sub>2</sub>O<sub>3</sub> film was formed on the Al surface, its protective nature against further oxidation caused non-ignition. In addition, T<sub>cr</sub> reduced with decreasing pressure and velocity of the streams. N<sub>2</sub> in the mixtures was found not to affect the ignition process. These experimental results are the same as those observed in our previous study on the ignition of

Al in CO<sub>2</sub> streams [10]. This leads to the conclusion that the ignition mechanism of Al without an original oxide coating in O<sub>2</sub>/N<sub>2</sub> mixture streams is basically identical with that in pure CO<sub>2</sub> streams. Thus the mechanism is as follows. Occurrence of the ignition depends on whether O<sub>2</sub> can diffuse to the Al surface or not. A diffusion flux of O<sub>2</sub> to the surface is controlled by the position of an Al vapor diffusion flame. When the vapor pressure of Al is significantly high, the gas phase reactions cause the formation of a fully developed flame. On the contrary, in the case of low vapor pressures, O<sub>2</sub> can easily diffuse toward the surface to form an Al<sub>2</sub>O<sub>3</sub> film on it, leading to non-ignition. This critical condition is determined by the critical non-dimensional ejection parameter  $-f_w$  [19];

$$-f_w = \frac{v_w}{\sqrt{2av}} \sim \frac{T_{Al} \cdot \dot{m}_{Al}}{\sqrt{P_m \cdot V_m}}$$

where  $a$  is the stagnation velocity gradient, and  $\nu$  is the kinematic viscosity of the O<sub>2</sub>/N<sub>2</sub> mixture flow.  $v_w$  is the ejection velocity from the surface.  $T_{Al}$  is the Al metal temperature, and  $\dot{m}_{Al}$  is the evaporation rate of Al, depending on the vapor pressure of Al and, in turn, on  $T_{Al}$ . If there exists a critical value of  $-f_w$  above which ignition occurs, the decrease of  $P_m$  and  $V_m$  facilitates ignition at lower  $T_{Al}$ . However, the result that the dependency of  $T_{cr}$  on pressure was greater than that on velocity as shown in Fig.2 is not explained by this equation. This requires further studies.

#### 4.2.2 With an original oxide coating

Small particles and wires of Al are rapidly heated before an appreciable deposit of Al<sub>2</sub>O<sub>3</sub> on their surfaces, leading to a progressive self-acceleration of heating due to the reactions

between Al and oxidizer. The self-acceleration causes ignition at much lower temperatures than the melting point [1,4]. Merzhanov et al. [4] reported that the ignition temperature of small wires decreased with increasing the heating power, that is, the heating rate. In the present experiment, however, the  $H_r$  attained was two orders in magnitude smaller than that obtained for small particles and wires. The estimated oxide thickness of present Al samples using the Merzhanov equation [4] became about 50-100  $\mu\text{m}$  before ignition, which was too thick for self-heat because of the protective nature of  $\text{Al}_2\text{O}_3$ . In fact, in the present experiment temperature runaways did not occur before ignition. Therefore, another breaking mechanism of an original oxide coating at lower temperatures must be considered.

The vapor pressure of Al is excluded from the mechanism due to sufficiently low values in the range from 1600 to 2000 °C. There was an interesting fact that the breaking always appeared on the circumference of the Al surface, which corresponded to the corner of the original Al sample rod. This implies that a mechanical tension force between the surface tension of liquid Al at the edge of the sample holder and an electromagnetic force introduced by the high frequency heater may stretch an original oxide film to break at the corner part. This mechanism can explain observed experimental results. Unfortunately, if the mechanism is true,  $T_{ig}$  obtained here was peculiar to the present experimental apparatus. Even so, it is really true for Al with an original oxide coating that ignition can occur above about 1600 °C at the instant when the coating breaks by starting gas-phase reactions close to the surface.

## 5. Conclusions

(1) The critical spontaneous ignition temperatures of Al samples without an original coating in  $O_2/N_2$  (20/80) mixture streams were lower than the melting point of  $Al_2O_3$ . They decreased with reduction in pressure and velocity of the streams. The formation of an  $Al_2O_3$  film on the surface caused non-ignition. During combustion, Al had a clean surface with a diffusion flame of Al vapor with  $O_2$ . The  $N_2$  in the mixtures did not affect the ignition and combustion process due to much less reactivity of Al with  $N_2$ .

(2) When the Al surface was covered with an original oxide coating, ignition occurred in the gas phase at the instant of the breaking of the coating. The combustion process was essentially identical to that without an original oxide coating.

(3) The combustion mechanism for the  $Al-O_2/N_2$  system is developed, including the surface and gas-phase reactions producing Al vapor,  $AlO$ ,  $Al_2O$ ,  $AlO_2$ ,  $O$  and condensed  $Al_2O_3$ .

This work was supported by the Grants-in-Aid for Special Project Research of Tokyo Metropolitan Government and Scientific Research of the Ministry of Education, Japan. The authors would like to express their thanks to Mr. Fukuchi, A. and Mr. Yoshida, T. for their cooperation in conducting the experiment.

## References

1. Friedman, R. and Macek, A., *Ninth Symposium (International) on Combustion*, Academic Press, 1963, p.703.
2. Brzustowski, T. A. and Glassman, I., *Heterogeneous Combustion* (Wolfhard et al, Ed.), Academic Press, 1964, Vol. 15, p.41.
3. Wilson, JR. R. P. and Williams, F. A., *Thirteenth Symposium (International) on Combustion*, The Combustion Institute, Pittsburgh, 1971, p.833.
4. Merzhanov, A. G., Grigorjev, Yu. M. and Galchenko, Yu. a., *Comb. Flame* 29: 1-14 (1977).
5. Laurendeau, N. M. and Glassman, I., *Combust. Sci. Tech.* 3: 77-82 (1971).
6. Brzustowski, T. A. and Glassman, I., *Heterogeneous Combustion* (Wolfhard et al, Ed.), Academic Press, 1964, Vol.15, p.177.
7. Kashireninov, O. E., *Pure. and Appl. Chem.* 62, No.5: 851-859 (1990).
8. Fontijn, A., *Combust. Sci. Tech.* 50: 151-162 (1986).
9. Yuasa, S. and Isoda, H., *Twenty-Second Symposium (International) on Combustion*, The Combustion Institute, Pittsburgh, 1989, p.1635.
10. Yuasa, S. Sogo, S. and Isoda, H., *Twenty-fourth Symposium (International) on Combustion*, The Combustion Institute, Pittsburgh, 1992, p.1817.
11. South, R. and Hayward, B. M., *Combust. Sci. Tech.* 12: 183-195 (1976).
12. Markstein, G. H., *AIAA Journal* 1: 550-562 (1963).
13. Newman, R. N. and Payne, J. F. B., *Combustion and Flame* 68: 31-41 (1987).

14. Law, C. K., *Combust. Sci. Tech.* 7: 197-212 (1973).
15. *JANAF Thermochemical Tables*, 2nd ed., The Dow Chemical Company, Michigan, 1974, 1975, 1978, 1982.
16. Henderson, C. B., *Combust. Sci. Tech.* 1: 275-278 (1970).
17. King, M. K., *Seventeenth Symposium (International) on Combustion*, The Combustion Institute, Pittsburgh, 1979, p.1317.
18. Gordon, S. and McBride, B., *Computer Program for Calculation of Complex Chemical Equilibrium Compositions, Rocket Performance, Incident and Reflected Shocks, and Chapman-Jouguet Detonations*, NASA SP-273, 1971.
19. Tsuji, H. and Yamaoka, I., *Eleventh Symposium (International) on Combustion*, The Combustion Institute, Pittsburgh, 1967, p.979.

Figure captions

Fig.1. Schematic of experimental apparatus.

Fig.2. Variation of critical ignition temperature for the case without an original oxide coating:

- (1) with ambient pressure at  $V_m=2$  m/s,
- (2) with  $O_2/N_2$  stream velocity at  $P_m=8$  kPa.

Fig.3. Time variation of an Al sample with an original oxide coating leading to ignition:  $P_m=8$  kPa,  $V_m=2$  m/s,

$T_{ig}=1934$  °C,  $Hr=2.90$  °C/s.

- (1) Video photographs, (2) Emission spectra.

Fig.4. Variation of ignition temperature with heating rate at  $P_m=8$  and 41.3 kPa, and at  $V_m = 2$  m/s for the case with an original oxide coating.

Fig.5. A direct photograph of a burning Al cylinder with deposits on the surface:

$T_{ig}=1703$  °C,  $Hr=3.51$  °C/s,  $P_m=21.3$  kPa,  $V_m=2$  m/s.

Fig.6. Filtered photographs of a burning Al (1) and corrected emission intensity distributions (2):

$T_{in}=1885$  °C,  $P_m=8$  kPa,  $V_m=2$  m/s, after ignition

20 sec. (a) Al emission=396 nm,  $\Delta\lambda=15$  nm;

(b) AlO emission=487 nm,  $\Delta\lambda=12$  nm;

(c) Continuous emission  $> 700$  nm.

Fig.7. Schematic of an Al- $O_2/N_2$  combustion mechanism postulated in this study.

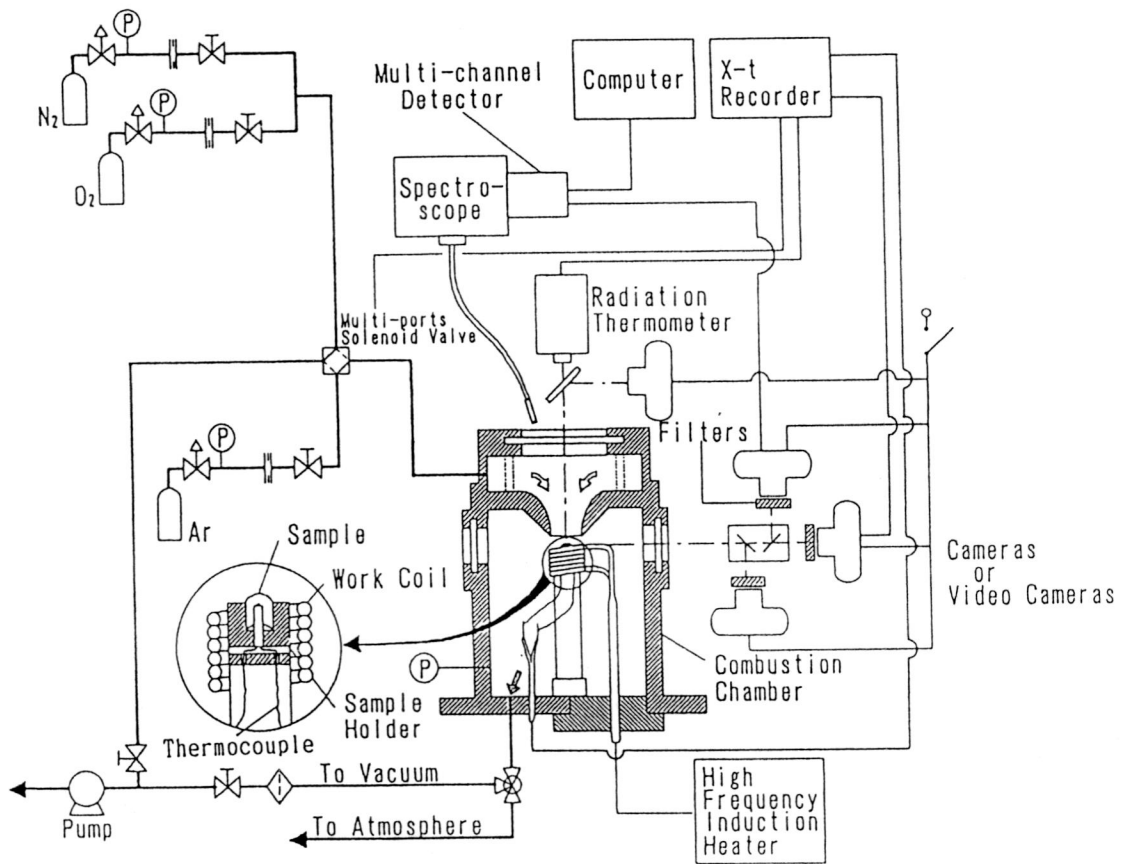


Fig.1. Schematic of experimental apparatus.

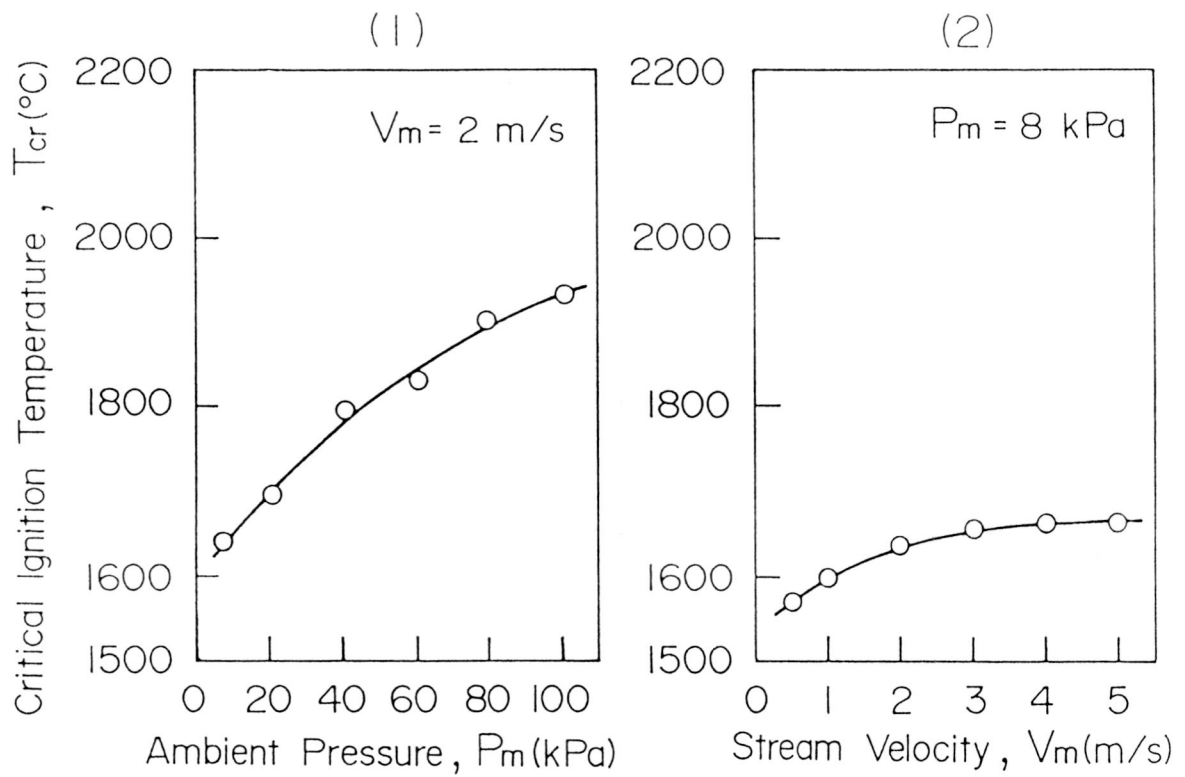


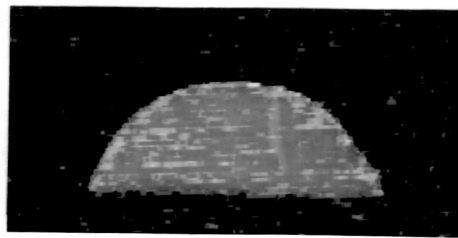
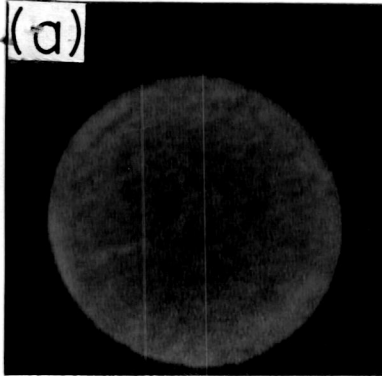
Fig.2. Variation of critical ignition temperature for the case without an original oxide coating:  
 (1) with ambient pressure at  $V_m = 2 \text{ m/s}$ ,  
 (2) with  $O_2/N_2$  stream velocity at  $P_m = 8 \text{ kPa}$ .

(1)

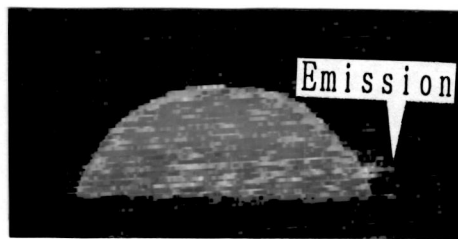
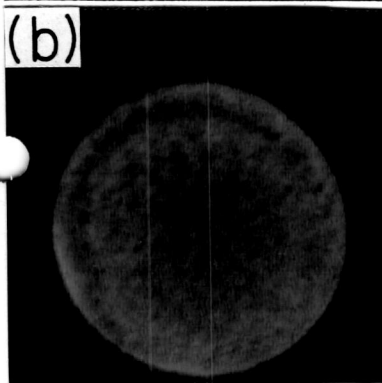
(2)

Top view

Side view



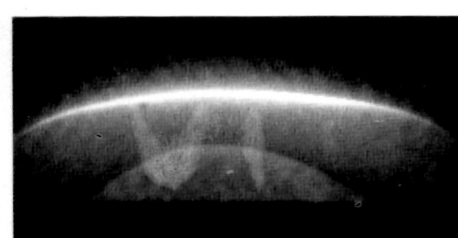
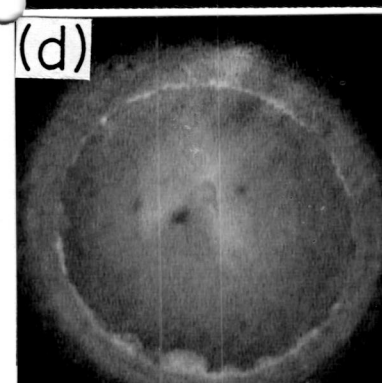
Just Before Ignition



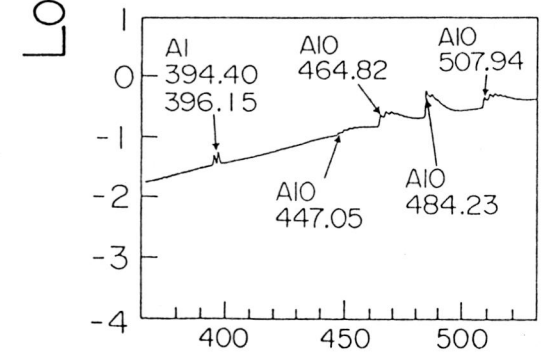
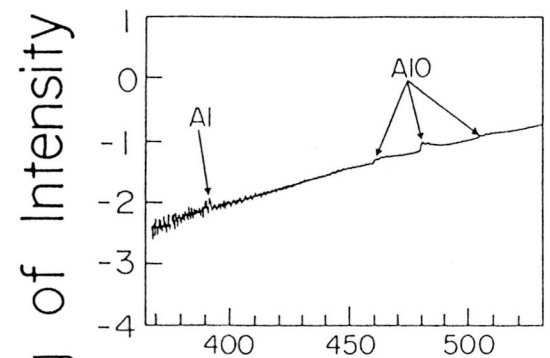
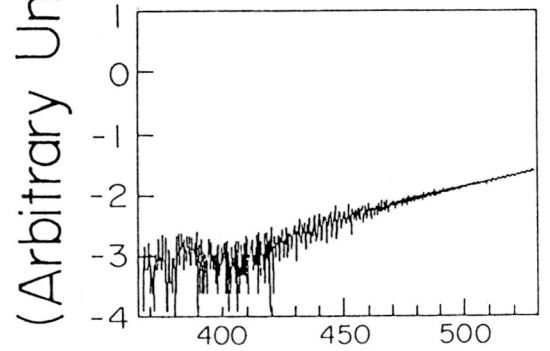
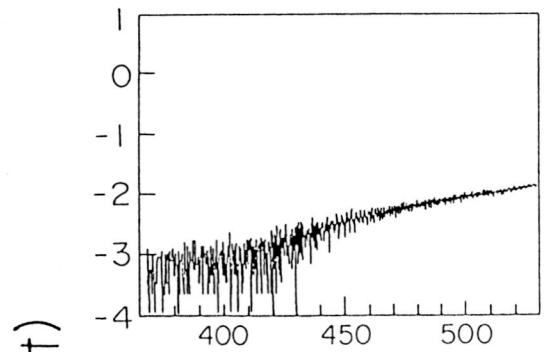
Ignition,  $t=0$  sec



$t=0.92$  sec



$t=11.18$  sec



Log of Intensity, (Arbitrary Unit)

Wave Length, (nm)

Fig.3. Time variation of an Al sample with an original oxide coating leading to ignition:  $P_m=8$  kPa,  $V_m=2$  m/s,  $T_{ig}=1934^\circ\text{C}$ ,  $H_r=2.90^\circ\text{C/s}$ .  
(1) Video photographs, (2) Emission spectra.

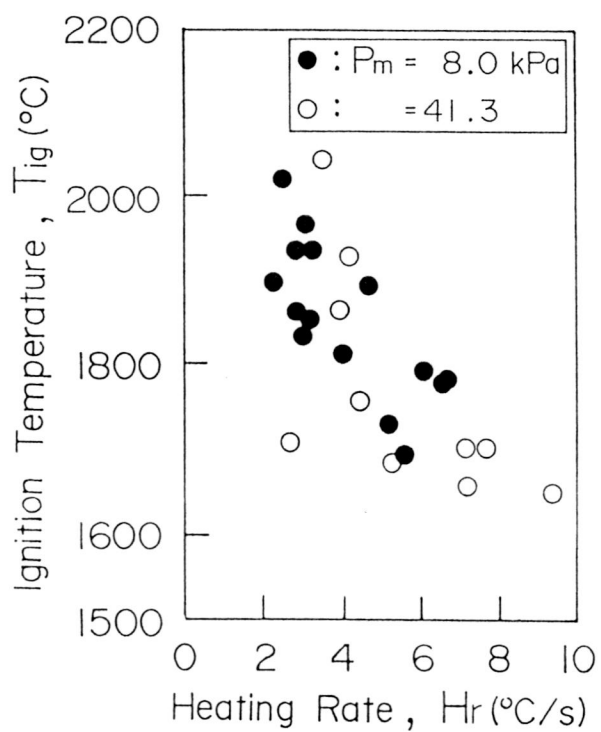


Fig.4. Variation of ignition temperature with heating rate at  $P_m=8$  and 41.3 kPa, and at  $V_m = 2$  m/s for the case with an original oxide coating.

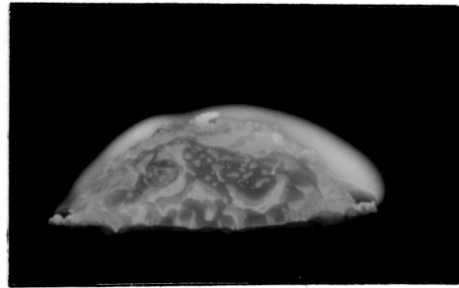


Fig.5. A direct photograph of a burning Al cylinder with deposits on the surface:

$T_{ig}=1703$  °C,  $Hr=3.51$  °C/s,  $P_m=21.3$  kPa,  $V_m=2$  m/s.

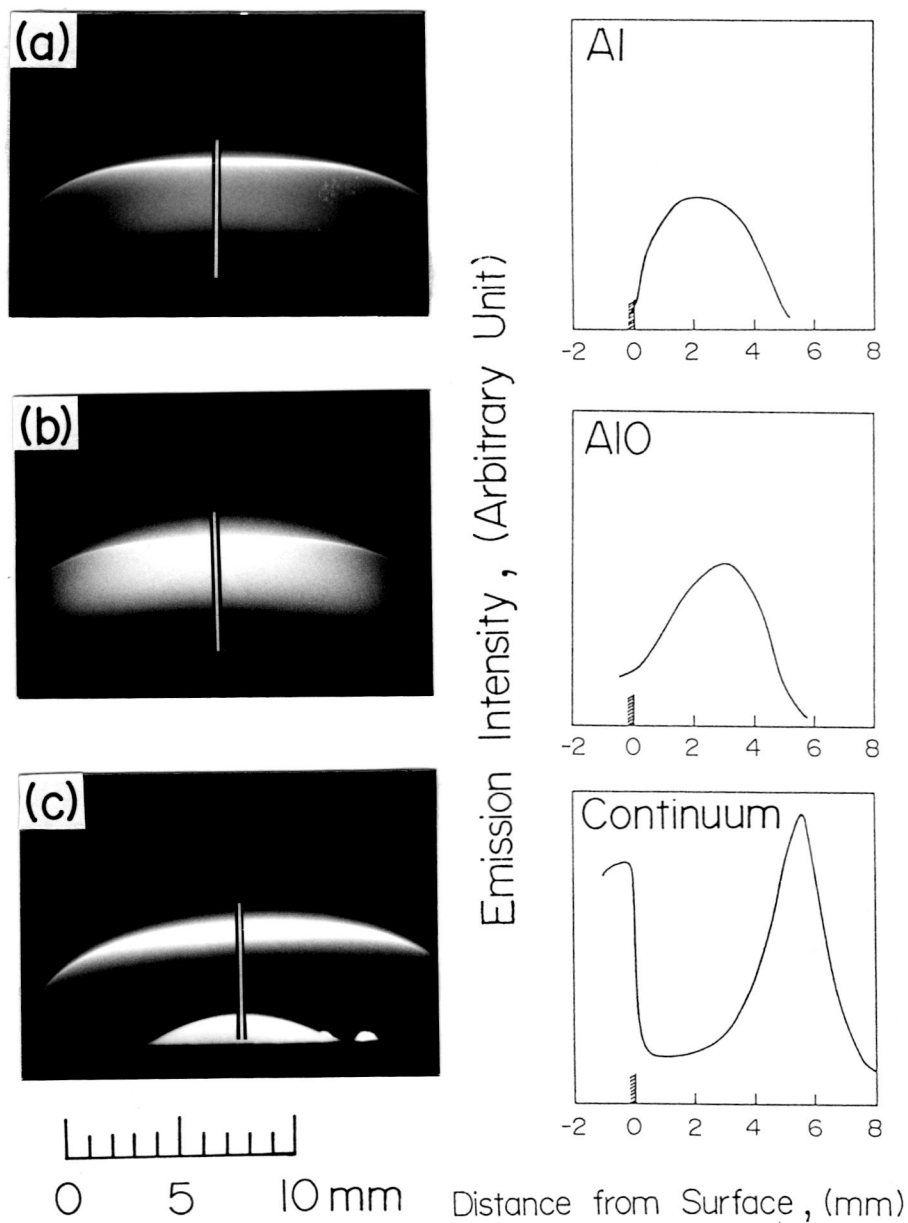


Fig. 6. Filtered photographs of a burning Al (1) and corrected emission intensity distributions (2):  $T_{in}=1885^{\circ}\text{C}$ ,  $P_m=8\text{ kPa}$ ,  $V_m=2\text{ m/s}$ , after ignition 20 sec. (a) Al emission=396 nm,  $\Delta\lambda/2=15\text{ nm}$ ; (b) AlO emission=487 nm,  $\Delta\lambda/2=12\text{ nm}$ ; (c) Continuous emission  $> 700\text{ nm}$ .

Surface Reactions

①, ②

Gas-Phase Reactions

③ ~ ⑧

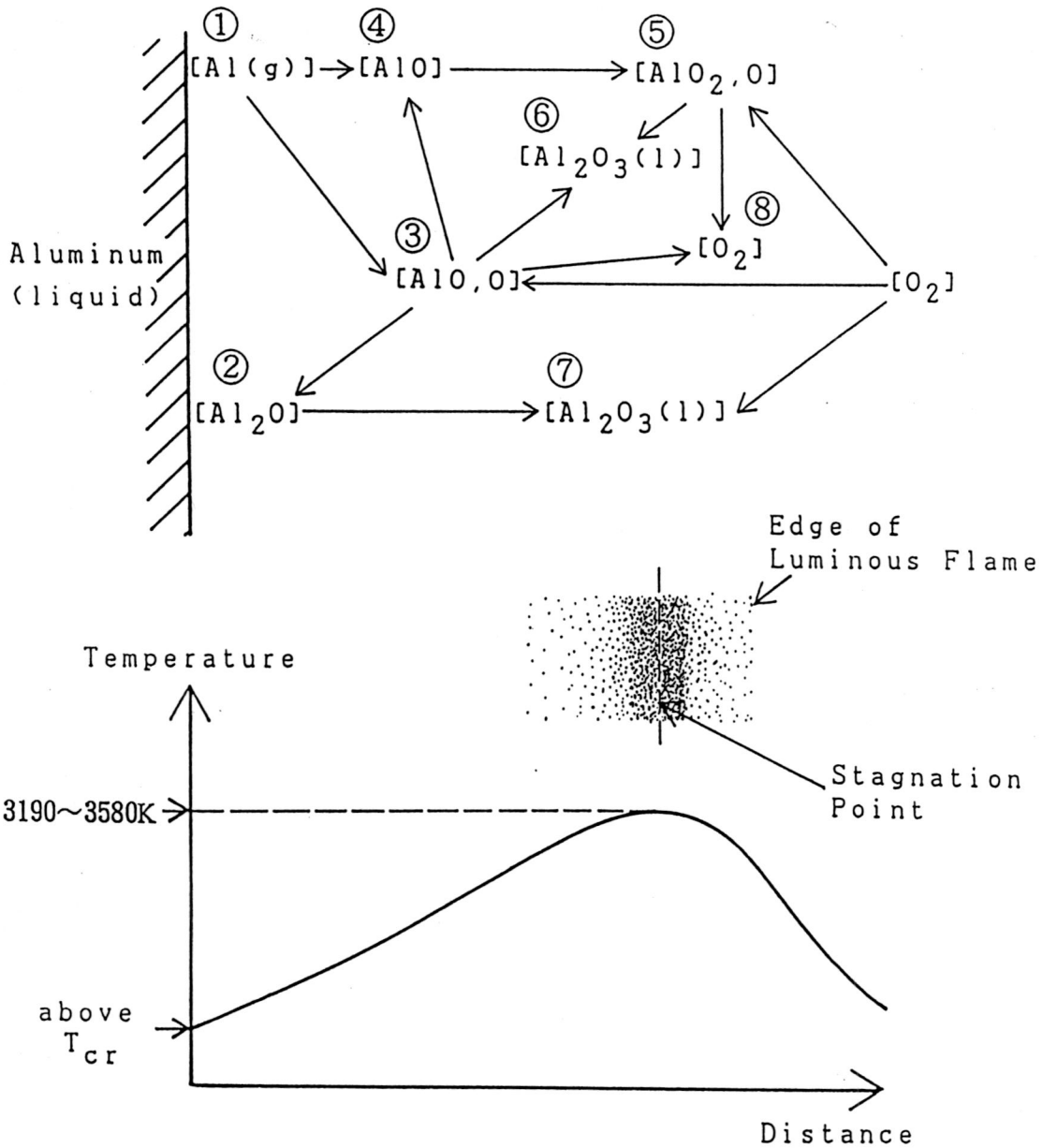


Fig.7. Schematic of an Al-O<sub>2</sub>/N<sub>2</sub> combustion mechanism postulated in this study.